# A Self-adaptive EM-HMRF Image Fusion Algorithm Based on Non-homogeneous Class and Direction

Guiqing HE* Yan ZHU
Northwestern Polytechnical University, Xi'an
E-mail: guiqing_he@nwpu.edu.cn Tel: +86-15802991311

*Abstact*—**Aim at classification-oriented feature-level fusion of remote sensing image, MRF is firstly introduced in this paper to build prior probability models for multiple object classes, and EM-HMRF scheme is introduced into image fusion by taking advantage of the equivalence relation between EM-HMRF and fuzzy classification algorithms. Secondly, focusing on how to select model parameter $b$ with self-adaptive character, a new selecting method is dirived. Then a self-adaptive EM-HMRF fusion algorithm is proposed basing non-homogeneous class and direction, which includes 2 centric and distributed-based fusion schemes. Theory analysis and experiment results show that our proposed algorithms with 2 fusion schemes can not only improve the classification accuracy but also enhance the ability to anti-interference, and they have the different advantages in various fusion systems for different applications, and thus improve the effectiveness of classification basing feature-level fusion of remote sensing image.**

## Ⅰ. INTRODUCTION

As the great development of space technology and remote sensing technology, earth observation data have a big increase from different sources and with distinct characteristics. At the same time, demands of the consumers are being transformed from static non real-time to dynamic real-time. However, the huge data above is a big challenge to real-time and quasi real-time data processing as well as data storing and transferring. The existing studies have shown that classification fusion treatment for multi-sensor remote sensing image fusion based on feature-level is the effective way to solve the problem of massive data and the contradiction between image storing and transferring[1-4].

Classification fusion treatment involves such two aspects primarily as classification and fusion strategies.

At present, in the research of image classification, MRF (Markov Random Field) model can typically build the prior distribution model, and it has attracted attention[1-12], especially G-MRF model (Gauss-MRF)[13-22]. But there is a shared MRF prior model parameter $b$ , which is selected manually by many times attempt, using in the whole image data. This is apparently not suitable for remote sensing image which has a complicated object features. Thus, aiming at classification fusion of multisource remote sensing image, MRF is introduced to model the prior distribution of a class, and different parameter $b$ should be used in MRF prior model to get better classification results. On the other hand, fusion process can achieve more precise, integrated and reliable estimation and description of the original scene than a single source image. Thus centralized-based and distributed-based fusion schemes are introduced in order to get better classification results.

Aim at classification-oriented feature-level fusion of remote sensing image, which has complicated object features, MRF is firstly introduced in this paper to build prior probability models for multiple object classes, Taking advantage of the equivalence relation between EM-HMRF(Expectation Maximization-Hierarchical Markov Random Field) and fuzzy classification algorithms, EM-HMRF algorithm is introduced into image classification fusion. This scheme adopts HMRF to model the images. And then employing the classical EM algorithm in incomplete data to substituting MAP (Maximum Aprior Probability) based on Bayes classification theory, parameters are estimated. Afterward, the selecting method of prior distribution model parameter $b$ is discussed as a key problem. Based on the former studies, the paper has proposed a self-adaptive EM-HMRF multi-sensor image fusion algorithm basing non-homogeneous class and direction, which includes 2 centric and distributed-based fusion schemes considering the different structures of feature-level fusion of multi-sensor images . The experimental results of synthetic images and real remote sensing images make it clear that both

Supported by NPU Foundation for Fundamental Research(NPU-FFR-JC20100215)

the two algorithms can obviously improve the classification precision and greatly strengthen the anti-interference for noise, and thus improve the effectiveness of classification basing feature-level fusion of remote sensing image.

## Ⅱ. HMRF IMAGE MODEL

The defined image $S$ is the two dimensional grid system of $A\times B$, and marked as $S=\{(i,j):1\le i\le A,1\le j\le B\}$. $N=\{N_{ij}:(i,j)\in S,N_{ij}\subseteq S\}$ is a neighborhood system on $S$. A random field distribution $X$ is the MRF(Markov Random Field) on grid structure $S$. If and only if it is a domain system $N$, $X$ meets the following conditions with regard to a neighborhood system $N$ [5]:

① $P(x)>0,\forall x\in c$

② $P(x_i|x_{S-\{i\}})=P(x_i|x_{N_i})$

where $c$ is the configuration space of $X$, $x_{N_i}$ is the random distribution of $x_i$ neighborhood domain.

Under the MRF model frame, applying a certain model to describe a whole real image sometimes can not reflect the complexity of remote sensing images. Therefore, HMRF model is usually adopted to describe an image in practical applications[6-8].

### A. Labeling Field Prior Model

The labeling field is a hidden random field and is used to describe pixel local related attributes. As the simple calculation of MLL (Multi-level Logistic), it is always used in model region and texture region[9-12]. Now according to the equivalence of MRF and GRF(Gibbs Random Field) described by Hamersley-Clifford theorem, the general equation of prior model is given in the following[5]:

$$p(x)=P(X=x)=\frac{1}{Z}\exp(-U(x)/T) \tag{1}$$

Where $Z=\sum_{x\in c}\exp(-U(x)/T)$ is probability distribution normalized factor, and is called partition function. $c$ is the configuration space of $X$. $T$ represents temperature. In energy function $U(x)=\sum_{c\in C}bV_c(x)$,

Where,

$$V_c(x)=\begin{cases}-1 & x_i=x_j\\ 1 & otherwise\end{cases}(1\le i\le A\times B,j\in N_i),$$

$V_c(x)$ is called potential function related to cluster $c$. $C$ is the collection of every cluster $c$. $b$ is the model parameter of labeling field.

### B. Image Field Model

Human visual system is very sensitive to the first order statistics (average value) and the second order statistics (variance and covariance) in images, but not sensitive to the third order statistics and higher order statistics. Thus, most of the present papers adopt a certain probability density function, which is Gaussian distribution, to model the image[13-22]. In the following, image field function is provided based on Gaussian density function. Suppose that pixel gray follows Gaussian distribution, and then the image model setting labeling field above as condition is described as:

$$f(y|w_s)=\frac{1}{\sqrt{2p}\,s_{w_s}}\exp[-\frac{(y-m_{w_s})^2}{2s_{w_s}^2}] \tag{2}$$

Gaussian model parameter is $q_{w_s}=(m_{w_s},s_{w_s})$, $m_{w_s},s_{w_s}$ is respectively the average value and variance in the domain of classification labeling $w_s$.

Till now, HMRF image model, which can use different image characteristics to realize target classification, has been set up. In the above image model, it is not only that pixel grey information is utilized; dependence relationship between neighborhood pixels called spatial information is also taken into consideration. Hence the model can make full use of the space and grey information provided by image data.

## Ⅲ. MAP-MRF FRAME

S. Geman and D. Geman have set up the image restoration and edge extraction MAP-MRF frame theory based on MRF and MAP[23]. When $\omega$ follows MRF distribution, MAP method is that Maximum Aprior Probability estimating $\hat{w}$ approximates image real classification $w$:

$$\hat{w}=\arg\max_{w\in c}P(w|y) \tag{3}$$

And $\chi$ is the configuration space of $w$.

According to Bayesian criterion:

$$P(w\,|\,y)=\frac{P(w,y)}{P(y)}=\frac{P(y\,|\,w)\cdot P(w)}{P(y)} \tag{4}$$

Where $y$ represents pixel gray observed. On the conditional of a certain image, denominator $P(y)$ in the above equation can be seen as a constant, which means that

$P(y)$ can be ignored in calculation. Consequently, MAP estimating $\hat{w}$ can be expressed as:

$$\hat{w} = \arg\max_{w \in c}(P(y \mid w) \cdot P(w)) \tag{5}$$

Apparently, in order to solve MAP-MRF problem, conditional probability $P(y|w)$ and model of $P(w)$, which is prior probability of $w$ , should be made sure firstly. And then optimal solution can be achieved according to MAP-MRF frame combining optimization algorithm.

The significant influence of classification method based on MAP-MRF is: every MRF formal description can be transformed into minimization problem of an energy function. Meanwhile, main problem of this algorithm is the complexity of combinatorial optimization algorithm, especially the remote sensing image treatment based on HMRF model, which is a difficult nonlinear optimization problem. Therefore, the later part in this paper will take the following calculation thought into consideration: model parameter estimating problem for image of unsupervised classification based on statistical model is transformed into model parameter estimating from incomplete data by EM algorithm.

## Ⅳ. EM ALGORITHM AND PATAMETER ESTIMATION

### A. EM Algorithm

When it refers to image classification field specifically, $y$ can be seen as the image gray observed, and $w$ represents image classification label, which can not be observed. Hence $y$ is called incomplete data, and $x = (y, w)$ is called complete data. A classical method to solve incomplete data problem is EM algorithm, which is a maximum likelihood method to recursively solve the incomplete data parameter estimating. The biggest advantage of this algorithm is that the convergence process is really smooth and not sensitive to disturbance. EM algorithm includes:

E step: $$Q(\Phi \mid \hat{\Phi}^{(t)}) = E[\log p(x \mid \Phi) \mid y; \hat{\Phi}^{(t)}] \tag{6}$$

M step: $$\hat{\Phi}^{(t+1)} = \arg\max_{\Phi} Q(\Phi \mid \hat{\Phi}^{(t)}) \tag{7}$$

Where $t$ is iteration times.

### B. Parameter Estimation

For the image model based on HMRF in this paper, parameter of bottom-level image field is $q_{w_s} = (m_{w_s}, s_{w_s})$ . EM algorithm can be used to find maximum likelihood estimation of model parameter. Comparatively, the calculation and selection of top-level labeling field model parameter $b$ is a difficult problem. Generally, repeated attempts and man-made selection is adopted to choose $b$ . And then the whole image data all use the selected $b$ [1,4,24,25]. Using the same parameter $b$ to calculate equals to the assumption that the awaiting classification images are homogeneous class and direction. In fact, for image data of different classes and different directions, using different $b$ can achieve a satisfactory classification results. And since there are many ground objects of diversified attributes in remote sensing images and there are noises in the process of image generating. Therefore, the study of non-homogeneous class and direction $b$ with self-adaptive character is of great significance.

To have a convenient equation in the next part, the equations of energy function based on MLL model and related potential function are changed into[3]:

$$U(x) = \sum_{k=1}^{K}\sum_{d=1}^{D}\sum_{c \in C} b_{k,d} V_c(x) \tag{8}$$

Where $V_c(x) = \begin{cases} -1 & x_i = x_j \\ 1 & otherwise \end{cases}$ , $b_{k,d}$ is the model parameter of labeling field. Subscript $k,d$ represents the different directions of class and neighborhood domain, and $D$ is direction number. For a 8-neighborhood domain system, direction number $D$ is 4, which means that there are four different directions $d = 0^o, d = 45^o, d = 90^o, d = 135^o$ . The four directions are corresponding to different clusters constructed by pixel pairs of various directions. Thus, the definition formula of non-homogeneous class and direction $b$ with self-adaptive character is given:

$$b_{k,d}^{t} = \sqrt{\frac{\sum_{i=1}^{M \times N}\left(\sum_{m \in N_i^d}\left(w_{ik}^t - w_{mk}^t\right)\right)^2}{N / c}} \tag{9}$$

$$k = 1, 2, \ldots, K, 1 \le i \le M \times N$$

Where $N_i^d$ represents $d$ direction neighborhood domain of pixel $i$ in image $S$. $w_{ik}^t, w_{mk}^t$ represents posterior probability of pixel $i$ and its $d$ direction neighborhood pixel $m$ belonging to class $k$ . Since posterior probability of pixel is the synthesis and extraction of spectral and space information of a certain pixel, the difference between posteriors of a pixel and its neighborhood domain pixel, which is of the same kind, can reflect the change of such two-dimensional information as image spectrum and space. Therefore, the definition of non-homogeneous class and direction $b_{k,d}$ gives a realer description of practical image data. In addition, $c$ in (9) stands for adjustment coefficient so that it will suit to the requirement of different image processing. For example, for image processing of severe noise contamination, $b$ is required to be bigger; conversely, for the one that needs to keep space details, $b$ is required to be smaller; otherwise $c=2$ in general. For the above reason, to set up the adjustment coefficient $c$ is reasonable and effective, which can make self-adaptive $b$ more suitable and general.

## Ⅴ. Remote Sensing Image Fusion Algorithm Based On Non-Homogeneous Class And Direction EM-hmrf Centralized And Distributed

### *A. EM-HMRF Classification Algorithm*

The process of image classification is giving every pixel a group of labels from the finite category centralized. The defined vector of pixel observation value is $y=\{y_s : s\in S\}$, and the defined vector of hidden value is $w=(w_{s_1}, w_{s_2}, \mathbf{L}, w_{s_{M\times N}})$, where $w_{s_i}$ is a vector to indicate the class of pixel $y_{s_i}$. If there are $K$ classes of images, then for a certain class of category $k$ $(1\le k\le K)$, $w_k = e_k$, $e_k$ stands for unit vector when component of number $k$ is 1 and other components are 0. $\Phi=(\Phi_y, \Phi_w)$ stands for parameter set, $\hat{w}_{ik}^{t}$ represents membership degree estimating value of pixel $i$ belonging to class $k$ at number $t$ iterative procedure,

Where, $\sum_{k=1}^{K} \hat{w}_{ik}^{t} = 1$, 且 $0 \le \hat{w}_{ik}^{t} \le 1$.

Now the realization steps of EM-HMRF classification algorithm provided by Zhang[14] is offered in the following:

Step 1, initialization process: to set up initial class labeling, $\hat{w}^0 = \{\hat{w}_{ik}^0 \mid i=1,2,\mathbf{L}, M\times N; k=1,2,\mathbf{L}, K\}$; to set up initial parameter, $\hat{\Phi}_k^0 = (\hat{\Phi}_{y,k}^0, \hat{\Phi}_{w,k}^0) = (\hat{m}_k^0, \hat{s}_k^0, 0)$; to set up iteration times, $t=0$.

Step 2, to achieve estimating parameter of image field by EM algorithm,

$$\hat{m}_k^t = \frac{1}{\hat{N}_k^{t-1}} \sum_{i=1}^{M\times N} \hat{w}_{ik}^{t-1} y_i \tag{10}$$

$$\hat{s}_k^t = \sqrt{\frac{1}{\hat{N}_k^{t-1}} \sum_{i=1}^{M\times N} \hat{w}_{ik}^{t-1} (y_i - \hat{m}_k^t)^2} \tag{11}$$

Where $\hat{N}_k^{t-1} = \sum_{i=1}^{M\times N} \hat{w}_{ik}^{t-1}$.

Step 3, to calculate estimating value of labeling field parameter $b$, which is of non-homogeneous class and direction, by (9).

Step 4, to scan whole image $i=1,2,\mathbf{L}, M\times N$, and calculate $\hat{w}_{ik}^t$ according to (14),

$$\begin{aligned}\hat{w}_{ik}^t &\overset{\Delta}{=} f(w_i = e_k \mid y; \hat{\Phi}^{t-1}) \\ &= \frac{f(y_i \mid w_i = e_k; \hat{\Phi}^{t-1})\, f(w_i = e_k; \hat{\Phi}^{t-1})}{\sum_{j=1}^{K} f(y_i \mid w_i = e_j; \hat{\Phi}^{t-1})\, f(w_i = e_j; \hat{\Phi}^{t-1})}\end{aligned} \tag{12}$$

In (12), conditional probability density function $f(y_i \mid w_i = e_k)$ is showed in (2), $w$ is a MRF and follows Gibbs distribution. And according to mean field approximation theory by Zhang[14,15], there is the equation:

$$f(w_i = e_k) = \frac{\exp[\hat{b}_{k,d}^t \hat{d}_i^{t-1}(k)]}{\sum_{k=1}^{K} \exp[\hat{b}_{k,d}^t \hat{d}_i^{t-1}(k)]} \tag{13}$$

Where, $\hat{d}_i^{t-1}(k) = \sum_{j\in N_i} \hat{w}_j^{t-1}(k)$, $\hat{b}_{k,d}^t$ is parameter estimating value in step 3. Then, to substitute (13) and (2) into (12), (14) can be achieved:

$$\hat{w}_{ik}^t = \frac{\exp[b\hat{d}_i^{t-1}(k) - \ln\sqrt{2p}\,\hat{s}_k^{t-1} - \frac{(y_i - \hat{m}_k^{t-1})^2}{2(\hat{s}_k^{t-1})^2}]}{\sum_{k=1}^{K} \exp[b\hat{d}_i^{t-1}(k) - \ln\sqrt{2p}\,\hat{s}_k^{t-1} - \frac{(y_i - \hat{m}_k^{t-1})^2}{2(\hat{s}_k^{t-1})^2}]}$$
$$k=1,2,\mathbf{L}, K, 1\le i\le M\times N \tag{14}$$

Step 5, if the change of parameter is smaller than the pre-supposed threshold, or iterative times reach pre-supposed value, then iteration is over. And it turns to step 6, otherwise it returns to step 2 and set up iterative times $t=t+1$.

Step 6, at every pixel $i=1,2,\mathbf{L}, M\times N$, according to $w_i^* = \arg\max_k \hat{w}_{ik}^{end}$, corresponding category labeling is given to every pixel. $\hat{w}_{ik}^{end}$ stands for the estimation of class labeling when iteration is over.

Obviously, every pixel $y_i$ in image makes a "soft decision" for all classes, which depicts similarity degree between pixel and every category. If it uses "hard decision" instead of "soft decision" in the step of the former iteration in EM algorithm, the algorithm is degenerated as unsupervised ICM iterative algorithm offered by Besag[14].

### *B. EM-HMRF Centric and Distributed-based Remote Sensing Image Fusion Algorithm Basing Non-homogeneous Class and Direction*

According to related theory of data fusion, distributed and centralized are two general structures in feature-level fusion. In this paper, based on non-homogeneous class and direction $b$ with self-adaptive character, 2 EM-HMRF centralized and distributed image fusion algorithms are presented. And there are advantages and disadvantages in the two types of fusion. In practical application, suitable fusion model should be chosen according to system conditions and processing requirements.

#### *(A). Centralized-based Fusion*

During data characteristic fusion of multi-sensor, if there are images of $P$ sources in front end and image data of various sources are independent from each other, then joint probability of front end image in fusion model will be represented as the product of $P$ conditional probabilities. Thus, the process of EM-HMRF fusion algorithm is not changed. And it only needs to modify (14) in step 4 into:

$$\hat{w}_{ik}^{t}=\frac{\exp\{\hat{b}_{k,d}^{t-1}\hat{d}_i^{t-1}(k)-\sum_{p=1}^{P}[\ln\sqrt{2p}\,\hat{s}_{p,k}^{t-1}+\frac{(y_{p,i}-\hat{m}_{p,k}^{t-1})^2}{2(\hat{s}_{p,k}^{t-1})^2}]\}}{\sum_{k=1}^{K}\exp\{\hat{b}_{k,d}^{t-1}\hat{d}_i^{t-1}(k)-\sum_{p=1}^{P}[\ln\sqrt{2p}\,\hat{s}_{p,k}^{t-1}+\frac{(y_{p,i}-\hat{m}_{p,k}^{t-1})^2}{2(\hat{s}_{p,k}^{t-1})^2}]\}}$$

*Where*, $1\le p\le P, 1\le k\le K, 1\le i\le M\times N$

(15)

Additionally, every image needs to be estimated when parameter is reevaluated.

#### *(B). Distributed-based Fusion*

It needs to classify every image respectively in distributed fusion model based on non-homogeneous class and direction EM-HMRF model so as to get vector collection of dependency degree for $P$ images with respect to class NO. $k(1\le k\le K)$. In fusion node, membership degree vector of various images is fused according to the subsequent method. Now the gray value of pixel $i$ in $p(1\le p\le P)$ image is marked as $g_{p_i}$, membership degree vector achieved by non-homogeneous class and direction EM-HMRF algorithm is $w_{p_i}^{*}=\{w_{p_{i1}}^{*},w_{p_{i2}}^{*},\mathbf{L},w_{p_{iK}}^{*}\}$. $w_{p_ik}^{*}$ represents membership degree of pixel $i$ in $p$ image with respect to classification $k$. Then the gray value of pixel $i$ is calculated as:

$$g_{p_i}=\sum_{k=1}^{K}w_{p_{ik}}^{*}\hat{m}_{p_{ik}} \qquad (16)$$

Where $\hat{m}_{p_{ik}}$ stands for parameter (average value) estimating value of class $k$ after the classification of pixel $i$ in $p$ image. Applying average value method to fuse $p$ images at fusion node, gray value of image after fusion is:

$$g_{f_i}=\frac{1}{P}\sum_{p=1}^{P}g_{p_i} \qquad (17)$$

At last, the final result is achieved by non-homogeneous class and direction EM-HMRF classification of fused images.

### *C. Experiments and Analysis*

The prior knowledge of the classes in remote sensing images is usually unavailable. In order to testify the new proposed algorithm performance and demonstrate its advantages, two sets of experiments are set up in this paper. One employs an artificial image to evaluate the algorithm performance quantitatively, the other adopts real remote sensing for subjective evaluation based on observation.

Fig.1 is an artificially composed grey-scale image with size of 128×128 pixels, which can be classified into three classes according to the pixel values. Fig.2(a) and (b) are images with additive Gaussian White Noise $N(0,0.056)$、$N(0,0.149)$、$N(0,0.256)$.

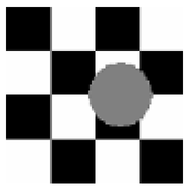

Fig. 1 Synthetic Image

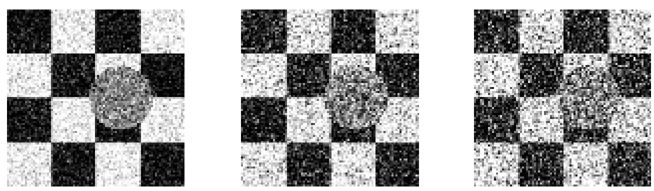

(a) Light Noise Contamination (b) middle Noise Contamination (c) heavy Noise Contamination

Fig. 2 Images with Additive Gaussian White Noise

We apply three iterative algorithms to Fig 2(a),(b) and (c):

SA algorithm[26], unsupervised ICM algorithm[27] and EM algorithm[14], denoted as SA-MAP-HMRF, UICM-MAP-HMRF and EM-HMRF respectively. The classification results are shown in Fig.3-5. We also apply the newly proposed non-homogeneous class and direction based EM-HMRF algorithm, both centric and distributed-based fusion schemes (CenF-EM-HMRF and DisF-EM-MAP -HMRF). The classification maps are shown in Fig.6-7. Sub-figure (a),(b) and (c) in the above mentioned figures are the results in light ,middle and heavy noise levels respectively. Because the test image is artificially composed, the test results can be compared and evaluated objectively and quantitatively. To guarantee the fairness, in the experiment, the same initial class tags are used and the fused image in the newly proposed algorithm is deduced from the two images with the given noise level.

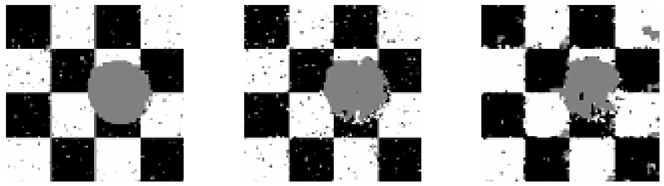

(a) (b) (c)

Fig.3 SA-MAP-HMRF

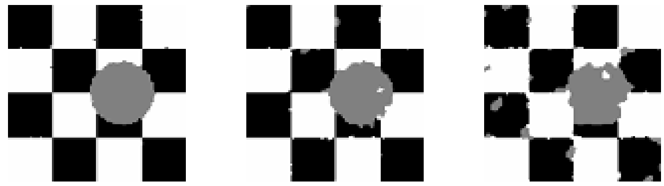

(a) (b) (c)

Fig.4 UICM-MAP-HMRF

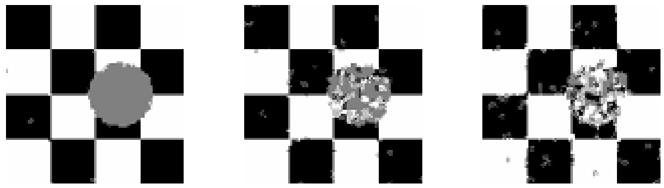

(a) (b) (c)

Fig. 5 EM-HMRF

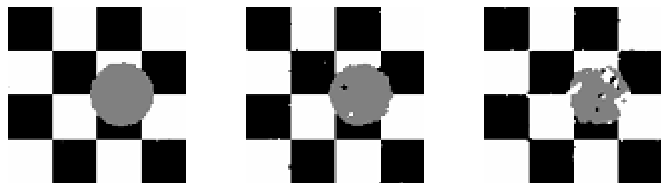

(a) (b) (c)

Fig. 6 CenF-EM-HMRF

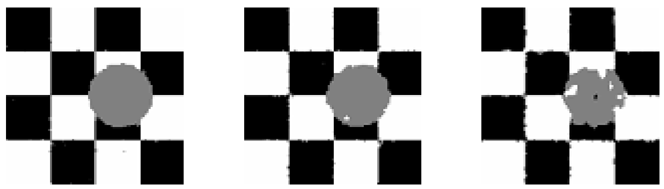

(a) (b) (c)

Fig. 7 DisF-EM-HMRF

Table Ⅰ lists the comparing results of classification accuracy and kappa parameter with light ,middle and heavy noise levels.

TABEL Ⅰ

COMPARING RESULTS OF CLASSIFICATION ACCURACY AND *kappa* PARAMETER

| | Light Noise Contamination | | Middle Noise Contamination | | Heavy Noise Contamination | |
|---|---|---|---|---|---|---|
| | Classification Accruacy (%) | ***kappa*** Parameter | Classification Accruacy (%) | ***kappa*** Parameter | Classification Accruacy (%) | ***kappa*** Parameter |
| **SA-MAP-HMRF** Algorithm | 97.638 | 0.95993 | 95.178 | 0.91778 | 92.285 | 0.86851 |
| **UICM-MAP-HMRF** Algorithm | 99.634 | 0.99373 | 98.749 | 0.97859 | 95.233 | 0.91942 |
| **EM-HMRF** Algorithm | 99.487 | 0.99123 | 95.447 | 0.92089 | 91.742 | 0.85498 |
| **CenF-EM-HMRF** Algorithm | 99.878 | 0.99791 | 99.097 | 0.98447 | 96.790 | 0.94411 |
| **DisF-EM-HMRF** Algorithm | 99.573 | 0.99270 | 98.602 | 0.97613 | 96.545 | 0.94080 |

Based on classification maps (Fig.3-7) and classification performance evaluation indices (Table Ⅰ), the following conclusions can be drawn:

*(A)* When the noise level is light, all the algorithms have high classification accuracy. While the noise level increases, the classification accuracy decreases, especially SA-MAP-HMRF and EM-HMRF algorithms. SA-MAP-HMRF algorithm adopts simulated annealing iteration strategy, and its iteration period and temperature drop processing are very long, therefore it's hard to get satisfied result only after several iterations. For EM-HMRF algorithm, because the same $b$ is used for the entire image, there is a tradeoff between the de-noising and detail preservation, especially in the high noise level case.

*(B)* UICM-MAP-HMRF algorithm has comparatively higher classification accuracy because of the ICM iteration it adopts. Compared to SA algorithm, ICM algorithm can converge rapidly. But it can not guarantee the convergence is the globally optimized solve. Therefore, the selection of initial values is critical for ICM algorithm. By choosing reasonable initial values, this algorithm can get satisfied classification results [28]. We adopts the theory of [28], sets ML estimation results as the initial values. Good results can be acquired.

*(C)* The newly proposed centric and distributed-based fusion schemes are capable of enhancing classification accuracy further. It's more evident in high noise level case. UICM-MAP-HMRF algorithm has large area of misclassification at the border. The newly proposed algorithms reduce the area of misclassification greatly and make the border more smooth and accurate. The higher the noise level, the higher the classification accuracy. This can be attributed to the merit of fusion model. The fusion model can reduce the uncertainty caused by noise in a single image and produce more accurate, complete and reliable estimation and judgment. Besides, the fusion center of centric fusion scheme can get the most complete information to produce result with high accuracy. The drawback is heavy calculation and cost, and the fusion result is also sensitive to the environment turbulence. The distributed-based fusion scheme depends on all the nodes, has higher real-time processing ability. It can be used for parallel computing to enhance classification rate and efficiency.

*(D)* Table Ⅱ lists the $b$ values in the newly proposed centric-based fusion schemes. Obviously, the $b$ values are class and direction non-homogeneous. In practical, the initial value of $b$ influences the classification results directly. With the increase of $b$, information in the neighborhood is strengthened. As a result, the ability of de-noising increases, while the image details are difficult to be preserved. In this paper, $b$ values in the compared algorithms are decided according to experience. In the newly proposed algorithms, the initial value of $b$ is set to 0 and then the value of $b$ in each iteration is calculated according to Eq.(9). From the subjective and objective evaluation based on Fig.3-7 and Table Ⅰ, it can be concluded that this strategy is more compatible with the real image features and can acquire more accurate classification results.

TABLE Ⅱ

THE RESULT $b$ VALUE OF CENTRIC-BASED FUSION SCHEME（$k,d$ respectively indicate different direction of class and neighborhood）

（**a**）Light Noise Contamination

| $\beta_{k,d}$ | $d=1$ | $d=2$ | $d=3$ | $d=4$ | $d=5$ | $d=6$ | $d=7$ | $d=8$ |
|---|---|---|---|---|---|---|---|---|
| $k=1$ | 2.3098 | 1.7348 | 2.3332 | 1.7319 | 2.3098 | 1.7348 | 2.3332 | 1.7319 |
| $k=2$ | 1.2193 | 1.0888 | 1.2479 | 1.0914 | 1.2193 | 1.0888 | 1.2479 | 1.0914 |
| $k=3$ | 2.2664 | 1.6610 | 2.2649 | 1.6284 | 2.2664 | 1.6610 | 2.2649 | 1.6284 |

（**b**）Middle Noise Contamination

| $\beta_{k,d}$ | $d=1$ | $d=2$ | $d=3$ | $d=4$ | $d=5$ | $d=6$ | $d=7$ | $d=8$ |
|---|---|---|---|---|---|---|---|---|
| $k=1$ | 2.2702 | 1.7011 | 2.2756 | 1.6439 | 2.2702 | 1.7011 | 2.2756 | 1.6439 |
| $k=2$ | 1.0322 | 0.8527 | 1.0053 | 0.8452 | 1.0322 | 0.8527 | 1.0053 | 0.8452 |
| $k=3$ | 2.2462 | 1.6603 | 2.2278 | 1.6040 | 2.2462 | 1.6603 | 2.2278 | 1.6040 |

( **c** ) Heavy Noise Contamination

| $\beta_{k,d}$ | $d=1$ | $d=2$ | $d=3$ | $d=4$ | $d=5$ | $d=6$ | $d=7$ | $d=8$ |
|---|---|---|---|---|---|---|---|---|
| $k=1$ | 2.2637 | 1.6728 | 2.2396 | 1.6673 | 2.2637 | 1.6728 | 2.2396 | 1.6673 |
| $k=2$ | 1.2537 | 1.0032 | 1.2026 | 0.9449 | 1.2537 | 1.0032 | 1.2026 | 0.9449 |
| $k=3$ | 2.3161 | 1.7284 | 2.2748 | 1.6841 | 2.3161 | 1.7284 | 2.2748 | 1.6841 |

Fig.8 is the experimental results of the newly proposed algorithms by using real remote sensing images. Fig.8(a)-(b) are SAR image and near infrared band of TM images with size of 300×300 pixels. Fig.8(c)-(d) are classification results of (a)-(b) by using UICM-MAP-HMRF respectively, and (e)-(f) are classification results of (a)-(b) by using EM-HMRF respectively. Fig.8(g)-(h) are classification results of the newly proposed CenF-EM-HMRF algorithm and DisF-EM -HMRF algorithm respectively. It can be classified into 6 classes according to the method of Iso-Grey Level Images.

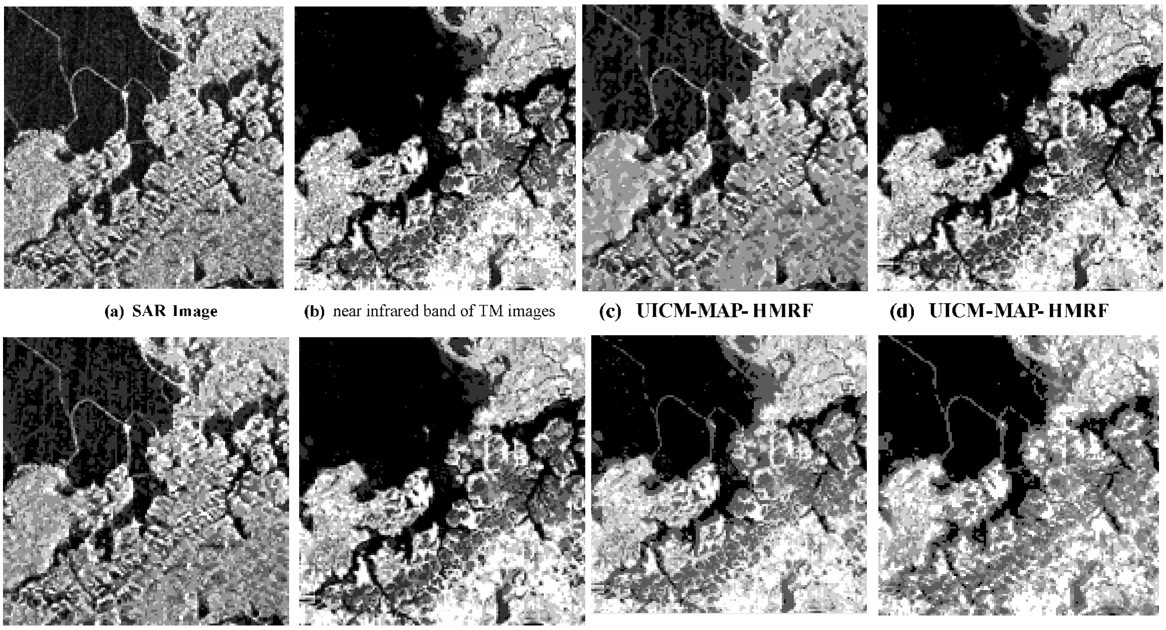

**(a) SAR Image** **(b)** near infrared band of TM images **(c) UICM-MAP- HMRF** **(d) UICM-MAP- HMRF**

**(e) EM-HMRF** **(f) EM-HMRF** **(g) CenF-EM- HMRF** **(h) DisF-EM - HMRF**

Fig. 8 Classification Result of Different Algorithm

SAR image has higher spatial resolution and abundant texture information, while TM images have higher spectral resolution and are more suitable for practical applications, such as classification and change detection. Therefore, we can integrate their own merits and complementary information to acquire more accurate, complete and reliable estimation and judgment than that from a single image. It can be observed from Fig.8 that there is more detailed information in (g) and (h) than that in TM image, because the features are abstracted from SAR image. On the other hand their classification accuracy is higher than that of SAR image, because the information from TM images. The newly proposed algorithms take both texture features in SAR image and spectral information in TM into consideration, to greatly enhance the classification accuracy. In practical, fusion scheme model can be selected according to calculation speed, classification accuracy and calculation cost.

## Ⅵ. CONCLUSION

MRF model can improve classification accuracy via pixel local related attributes. HMRF can reflect the complexity of remote sensing images much more. EM algorithm is a classical method to solve incomplete data parameter estimating in image processing of unsupervised classification. Prior distribution model parameter $b$ is calculated by Maximum Aprior Probability, and it is with self-adaptive character, non- non-homogeneous class and direction attributes. Thus the above parameter $b$ gives a realer description of practical remote sensing image data with complexity character. Based on the former studies, in order to improving the target identification, Markov random field is introduced in the target fusion process to build prior probability model of a class. Then aiming at how to select model parameter $b$ , an EM-HMRF feature-level fusion algorithm is proposed basing non-homogeneous class and direction. And then, 2 centric and distributed-based fusion schemes are derived, which consider the different structures of feature-level fusion for multi-sensor images. The simulations show that the 2 new fusion algorithms can not only improve the classification accuracy but also enhance the ability to anti-interference, and they have the different advantages. The 2 new schemes can be used in various fusion systems for different applications and thus improve the effectiveness of classification basing feature-level fusion of remote sensing image. Furthermore, the proposed classification-oriented fusion algorithm in this paper has a great enlightening meaning and reference value for this multisource remote sensing image classification fusion strategy.

## REFERENCES


[1] Blekas K, Likask A, Galatsanos N P, et al. A Spatially Constrained Mixture Model for Image Segmentation[J]. IEEE Transactions on Neural Networks, 2005, 16(2): 494-498

[2] Yakoub B, Farid M.Gaussian Process Approach toRemote Sensing Image Classification[J]. IEEE Transactions on Geoscience and Remote Sensing, 2010, 48(1): 186-197

[3] Nikou C, Galatsanos N P, Likas A C. A Class-Adaptive Spatially Variant Mixture Model for Image Segmentation[J]. IEEE Transactions on Image Processing, 2007, 16(4): 1121-1130

[4] Zhang Y Y, Brady M, Smith S. Segmentation of Brain MR Images through a Hidden Markov Random Field Model and the Expectation-Maximization Algorithm[J]. IEEE Transactions on Medical Image, 2001, 20(1): 45-57

[5] Wai-Ki C, Michael K N. Markov Chains: Models, Algorithms and Applications[M]. Springer, 2006

[6] Dang M, Govaert G. Spatial Fuzzy Clustering Using EM and Markov Random Fields[J]. System Research and Information Systems, 1998, (8): 183-202

[7] Guo Xiao-wei, Tian Zheng, Liu Bao-li. A Fast Algorithm for Hidden Markov Tree Training in Image Denoising. Journal of Northwestern Polytechnical University, 2004, 22(4): 457-462

[8] Derin H, Elliott H. Modeling and Segmentation of Noisy and Textured Images Using Gibbs Random Fields[C]. IEEE Transaction on Pattern Analysis and Machine Intelligence, 1987, 9(1): 39-55

[9] Deng H, Clausi D A. Unsupervised Image Segmentation Using a Simple MRF Model with a New Implementation scheme[J]. Pattern Recognition, 2004, 37(12): 2323-2335

[10] Xu X, Li D, Sun H. Multiscale SAR Image Segmentation Using a Double Markov Random Field Model[C]. Proceedings of IEEE 7th International Symposium on Signal Processing and its Applications, 2003,1: 349-352

[11] Manjunath B S, Chellappa R. A Markov Random Field Model-based Approach to Image Interpretation[J]. IEEE Transactions on Pattern Analysis and Machine Intelligence, 1992,14(6): 606-615

[12] Yamron J P, Carp I, Gillick L, et al. A Hidden Markov Model Approach to Text Segmentation and Event Tracking[C]. Proceedings of the IEEE International conference on Acoustics, Speech and Signal Processing, 1998, 1: 333-336

[13] LI Xu-chao, ZHU Shan-an. A Survey of the Markov Random Field Method for Image Segmentation. Journal of Image and Graphics, 2007, 12(5): 789-798

[14] Zhang J, Modestino J W, Langan D A. Maximum-Likelihood Parameter Estimation for Unsupervised Stochastic Model-Based Image Segmentation[C]. IEEE Transactions on Image Processing, 1994, 3(4): 404-420

[15] Zhang J. The Mean Field Theory in EM Procedures for Markov Random Fields[J]. IEEE Transactions on Signal Processing, 1992, 40(10): 2570-2583

[16] Zhang Y, Brady M, Smith S. Segmentation of Brain MR Images through a Hidden Markov Random Field Model and the Expectation Maximization Algorithm[J]. IEEE Transactions on Medical Imaging, 2001, 20(1): 45-47

[17] Wang J P. Stochastic Relaxation on Partitions with Connected Components and Its Application to Image Segmentation[J]. IEEE Transactions on Pattern Analysis and Machine Intelligence, 1998, 20(6): 619-636

[18] Biemacki C, Celeux G, Govaert G. Assessing a Mixture Model for Clustering with the Integrated Completed Likelihood[J]. IEEE Transactions on Pattern Analysis and Machine Intelligence, 2000, 22(7): 719-725

[19] Comer M L, Delp E J. The EM/MPM Algorithm for Segmentation of Textured Images Analysis and Further Experimental Result[J]. IEEE Transactions on Image Processing, 2000, 9(10): 1731-1744

[20] YU Peng, ZHANG Zhen-long, HOU Zhi-qun. Textured Image Segmentation Based on Gauss Markov Random Field Mixture Model. ACTA Geodaetica et Cartographica Sinica, 2006, 35(3): 224-228

[21] LIU Xiao-yun, WANG Zhen-song, CHEN Wu-fan, et al. Remote Sensing Images Hierarchical Clustering Using Markov Random Field and Generalized Gaussian Mixture Models. Journal of Remote Sensing, 2007, 11(6): 838-844

[22] Chen Yun-jie, Wang Shun-feng, Wang Li. Brian MR Images Segmentation Based on Anisotropic Gibbs Random Field and

Gauss Mixture Model. Journal of Computer-Aided Design and Computer Graphics, 2007, 19(12): 1550-1563
[23] Geman S, Geman D. Stochastic Relaxation, Gibbs Distribution and the Bayesian Restoration of Images[J]. IEEE Transaction on Pattern Analysis and Machine Intelligence, 1984, 6(6): 721~741
[24] Won C S, Derin H. Unsupervised Segmentation of Noisy and Texture Image Using Markov Random Fields[J]. Graphical Models and Image Processing, 1992, 54(4): 308-328
[25] Zhang B B, Zhang C S, Yi X. Competitive EM Algorithm for Finite Mixture Models[J]. Pattern Recognition, 2004, 37(1):131-144
[26] Lankoacde O, Hayat M.M, Santhanam B. Speckle Reduction of SAR Images Using a Physically Based Markov Random Field Model and Simulated Annealing[C]. Proceedings of SPIE, 2005, 5808: 210-221
[27] ZHANG Cui, LI Su-dan, WANG Zheng-zhi. SAR Image Segmentation Based on Markov Random Field Model[J]. Remote Sensing Technology and Application, 2001, 16(1): 66-68
[28] Besag J. On the Statistical Analysis of Dirty Pictures[J]. Journal of Royal Statistical Society(B), 1986, 48(3): 259-302